Organic Electronics 35 (2016) 41–46

Contents lists available at ScienceDirect

Organic Electronics

journal homepage: www.elsevier.com/locate/orgel

3,7-Bis((*E*)-2-oxoindolin-3-ylidene)-3,7-dihydrobenzo[1,2-*b*:4,5-*b*′] dithiophene-2,6-dione (IBDT) based polymer with balanced ambipolar charge transport performance

Yinghui He, Jesse Quinn, Yunfeng Deng, Yuning Li*

Department of Chemical Engineering and Waterloo Institute for Nanotechnology (WIN), 200 University Ave W, Waterloo, Ontario, N2L 3G1, Canada

ARTICLE INFO

Article history:
Received 22 February 2016
Received in revised form
30 April 2016
Accepted 5 May 2016

Keywords:
Printed electronics
Polymer semiconductors
New acceptor building blocks
Organic thin film transistors
Ambipolar charge transport

ABSTRACT

A novel acceptor building block, 3,7-bis((*E*)-2-oxoindolin-3-ylidene)-3,7-dihydrobenzo[1,2-*b*:4,5-*b*′] dithiophene-2,6-dione (IBDT), is developed to construct a donor-acceptor polymer **PIBDTBT-40**. This polymer has favorable highest occupied molecular orbital (HOMO) and lowest unoccupied molecular orbital (LUMO) energy levels for balanced ambipolar charge transport. Organic thin film transistors (OTFTs) based on this polymer shows well-balanced ambipolar characteristics with electron mobility of 0.14 $cm^2 V^{-1} s^{-1}$ and hole mobility of 0.10 $cm^2 V^{-1} s^{-1}$ in bottom-gate bottom-contact devices. This polymer is a promising semiconductor for solution processable organic electronics such as CMOS-like logic circuits.

1. Introduction

Polymer semiconductors have been extensively studied as channel materials in organic thin film transistors (OTFTs) due to their good solution processability and mechanical robustness [1–3]. Different from unipolar p-type or n-type semiconductors, ambipolar semiconductors are able to transport both holes and electrons, allowing for certain new device designs such as single-component complementary metal oxide semiconductor (CMOS)-like circuits and ambipolar light emitting transistors [4–6]. The use of a single-component ambipolar polymer can significantly simplify the complicated patterning and fabrication processes for CMOS-like circuits [7]. Ambipolar light emitting transistors can integrate both the light-emission capability and the electrical current modulation in one single device architecture, which may enable the next generation of light-emitting devices [8]. For both single-component CMOS-like circuits and ambipolar light emitting transistors the semiconductor with balanced hole and electron charge transport characteristics is highly preferable [9]. To achieve balanced ambipolar charge transport characteristics, the frontier molecular orbital energy levels, i.e., the highest occupied molecular orbital (HOMO) and the lowest unoccupied molecular orbital (LUMO) of the polymer semiconductor are crucial. First, the HOMO and LUMO levels of the polymer semiconductor should have small and similar differences against the Fermi energy of the source contact to minimize and balance the injection barriers for electrons and holes, respectively [10]. In this regard, it is desired that the polymer has a small band gap (the difference between the HOMO and LUMO levels), while the Fermi level of the source electrode sits in between the LUMO and HOMO levels. Second, the energy levels of the polymer need to be lower than ca. −5.0 eV [11,12] for the HOMO and ca. −3.7~−4.0 eV [12–15] for the LUMO in order to achieve stable hole and electron transport, respectively. The common approach to delicately tune the energy levels of polymer semiconductors is to incorporate alternating donor–acceptor (D–A) structure in the polymer backbone, whereas the HOMO and LUMO levels of the polymers are primarily governed by an appropriate combination of the donor and acceptor building blocks, respectively [16,17]. However, available electron acceptor building blocks that are able to bring the LUMO level of polymers below ca. −3.7~−4.0 eV for stable and efficient electron transport are rare [18–21]. Hence, extensive effort has been made to discover new electron acceptor building blocks [22–24].

Recently we developed a new strong electron acceptor building block, (3*E*,7*E*)-3,7-bis(2-oxoindolin-3-ylidene)-benzo[1,2-*b*:4,5-*b*′]

* Corresponding author.
E-mail address: yuning.li@uwaterloo.ca (Y. Li).

http://dx.doi.org/10.1016/j.orgel.2016.05.003
1566-1199/

difuran-2,6(3*H*,7*H*)-dione (IBDF, Fig. 1), for D-A polymers for OTFTs [15,18,25–29]. Due to their deep-lying LUMO levels, IBDF-based polymers showed n-type dominant charge transport behavior with high electron mobility up to 1.74 $cm^2\ V^{-1}\ s^{-1}$ [26]. By replacing the benzodifurandione (BDF) core in IBDF with a less electron-withdrawing benzodipyrroledione (BDP), we developed another electron acceptor, IBDP (Fig. 1). Opposed to the IBDF-based polymers, the IBDP-based polymers showed p-type dominant charge transport behaviors with hole mobility as high as 1.92 $cm^2\ V^{-1}\ s^{-1}$ [30,31]. In this work, we changed the core unit to benzodithiophenedione (BDT) to successfully develop another new acceptor building block in this series, 3,7-bis((*E*)-1-2-oxoindolin-3-ylidene)-3,7-dihydrobenzo[1,2-*b*:4,5-*b*′]dithiophene-2,6-dione (IBDT, Fig. 1) and demonstrated that IBDT is a proper electron acceptor building block for making ambipolar polymers with well-balanced hole and electron mobilities.

2. Results and discussion

To probe how the sulphur atoms would impact the geometry and HOMO/LUMO levels of IBDT, we carried out a computational simulation on the model molecule, IBDT-Me with methyl substituents on nitrogen atoms (Figure S1, Supplementary Data). The calculated HOMO/LUMO levels are −5.64 eV/−3.46 eV, which are higher than those of IBDF-Me (−6.11 eV/−3.78 eV), but lower than those of IBDP-Me (and −5.52 eV/−3.44 eV) [30]. These results suggest that the IBDT-based polymers may exhibit ambipolar charge transport behavior. The simulations also gave the dihedral angle between the BDT core and the indolin-2-one ring to be ~14°, which turned out to be larger than those of IBDF-Me (~8°) and IBDP-Me (~10°). This is attributed to the twisting of the cyclic thioester ring due to the larger sulphur atoms. A detailed discussion can be found in the footnote of Table S1 (Supplementary Data).

The synthetic route to a new dibrominated IBDT monomer **3** is outlined in Scheme 1. Synthesis of 3,7-dihydrobenzo[1,2-*b*:4,5-*b*′]dithiophene-2,6-dione (**2**), the key precursor compound to the monomer **3**, was described only in one paper without much experimental details [32]. First benzo[1,2-*b*:4,5-*b*′]dithiophene was lithiated and then treated with tri-*n*-butyl borate to give **1**, which is essentially insoluble in common organic solvents. For the oxidation of **1**, we found that the amount of hydrogen peroxide and the reaction time are crucial. After optimization, compound **2** was obtained in a moderate yield of 61%. The aldol condensation of **2** with 6-bromo-1-(4-octadecyldocosyl)indoline-2,3-dione in refluxing toluene with a catalytic amount of *p*-toluenesulphonic acid afforded monomer **3** in 22% yield. Finally, an IBDT-based polymer **PIBDTBT-40** was synthesized via the Stille coupling reaction between **3** and 5,5′-bis(trimethylstannyl)bithiophene using $Pd_2(dba)_3$ and P(*o*-tolyl)$_3$ as the catalyst. The crude polymer was purified by Soxhlet extraction using acetone and hexanes to remove impurities and oligomers, and finally dissolved with chloroform. Besides chloroform, **PIBDTBT-40** is soluble in several other common solvents such as toluene, *m*-xylene, chlorobenzene, 1,2-dichlorobenzene, and 1,1,2,2-tetrachloroethane. The molecular weight and polydispersity (PDI) of this polymer were determined by high temperature gel permeation chromatography (HT-GPC) at 140 °C using 1,2,4-tricholorobenzene as the eluent and polystyrene as standards. A number averaged molecular weight (M_n) of 21.0 kDa and a polydispersity index (PDI) of 2.3 were obtained. The thermal stability of the polymer was characterized by thermogravimetric analysis (TGA) (Figure S5, Supplementary Data). A decomposition temperature of ~300 °C for a 5% weight loss was found for **PIBDTBT-40**, which is lower than the analogues of IBDF- [26] and IBDP- [30] based polymers (~380 °C). This could be attributed to the less stable thioester groups in IBDT [33].

The adsorption spectra of **PIBDTBT-40** in dilute solution (~10^{-5} M in $CHCl_3$) and thin film are shown in Fig. 2a. Both absorption spectra showed a dual band absorption profile, where the high energy band originates from the π–π* transition of the IBDT unit and the- low energy band can be attributed to the D-A intramolecular charge transfer (ICT) [34]. The wavelength of absorption maximum (λ_{max}) was slightly blue-shifted from 806 nm in solution to 794 nm in the thin film, which might be due to H-aggregation of polymer chains in the solid state [35,36]. By taking the absorption onset, the optical band gap of the polymer thin film was calculated to be 1.23 eV. Fig. 2b shows the cyclic voltammetry (CV) diagrams of **PIBDTBT-40**, which exhibits reversible redox processes. The oxidative and reductive peaks originate from the donor (bithiophene) and the acceptor (IBDT) units, respectively. Within the applied bias range from −1.3 V to 1.4 V there are two readily distinguishable peaks in the oxidation and reduction processes, respectively, indicating that distinct multiple redox sites exist within this polymer. The HOMO and LUMO levels of **PIBDTBT-40** were calculated from the oxidation and reduction onsets of the CV diagrams to be −5.60 eV and −4.06 eV, respectively (Fig. 2b), which are favoured for both stable hole and electron transport. Compared with the HOMO/LUMO levels of its analogues IBDF and IBDP polymers **PIBDFBT-40** (−5.72 eV/−3.88 eV) and **PIBDPBT-24/12** (−5.60 eV/−3.71 eV) (Fig. 1), the trends disagree with results predicted for their monomer compounds by computer simulations, where both HOMO and LUMO levels of IBDT-Me are located between those of IBDF-Me and IBDP-Me. Particularly the LUMO level of **PIBDTBT-40** is even lower than that of **PIBDFBT-40**, but IBDT is predicted to be a weaker electron acceptor than IBDF. The band gap of organic semiconductors obtained using the CV method is often larger than that obtained from the UV–vis measurement, which is due to the exciton binding energy (E_b) that has a value as high as ca. 0.4–1 eV [37,38]. We noticed that E_b ($E_g^{CV} - E_g^{opt}$) for **PIBDTBT-40** (1.46 eV–1.23 eV = 0.23 eV) is much smaller than that of **PIBDFBT-40** (1.84 eV–1.31 eV = 0.53 eV) or **PIBDPBT-40**

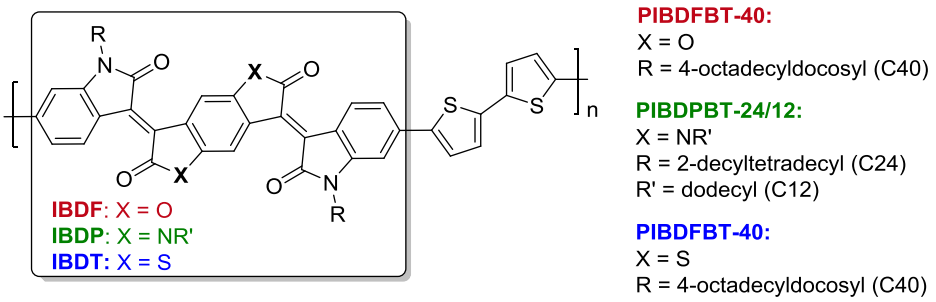

Fig. 1. IBDF, IBDP and IBDT building blocks and their polymers.

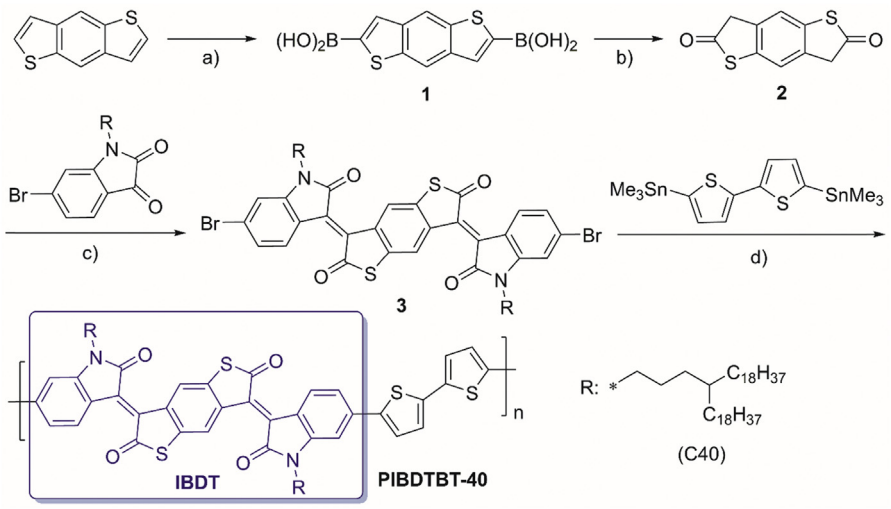

Scheme 1. Synthetic route to the brominated IBDT monomer **3** and **PIBDTBT-40**: a) Tetrahydrofuran/*n*-butyl lithium/−78 °C, tributyl borate/−78 °C to r.t.; b) Tetrahydrofuran/hydrogen peroxide/r.t.; c) Toluene/*p*-toluenesulphonic acid/reflux.; d) Chlorobenzene/P(*o*-tolyl)$_3$/Pd$_2$(dba)$_3$/130 °C.

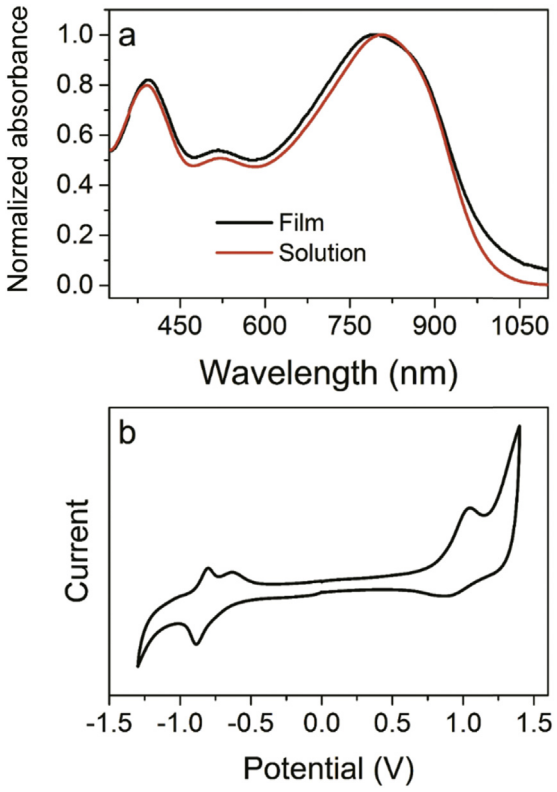

Fig. 2. a) The UV–Vis–NIR adsorption spectra of **PIBDTBT-40** in solution (chloroform) and in thin film. b) Cyclic voltammetry (CV) diagrams of a **PIBDTBT-40** film in a 0.1 M tetrabutylammonium hexafluorophosphate solution in acetonitrile using an Ag/AgCl reference electrode at a scan rate of 100 mV s^{-1}.

(1.89 eV−1.23 eV = 0.66 eV). Therefore, the small exciton binding energy of **PIBDTBT-40** appears to be the reason for its lower than expected LUMO level. A smaller exciton binding energy is beneficial for the exciton dissociation to reduce energy loss in the organic photovoltaics (OPVs) [39]. The decreasing exciton binding energy order observed for the three polymers, **PIBDPBT-40** > **PIBDFBT-40** > **PIBDTBT-40**, seems to be related to their different heteroatom (X) in the central core: N, O, and S. However, the reason for this observation is still unclear. It is interesting and worthwhile to investigate the behavior of these polymers in OPVs.

The charge transport performance of **PIBDTBT-40** was evaluated as a channel semiconductor in OTFT devices with a bottom-gate bottom-contact (BGBC) configuration. The device substrate is an

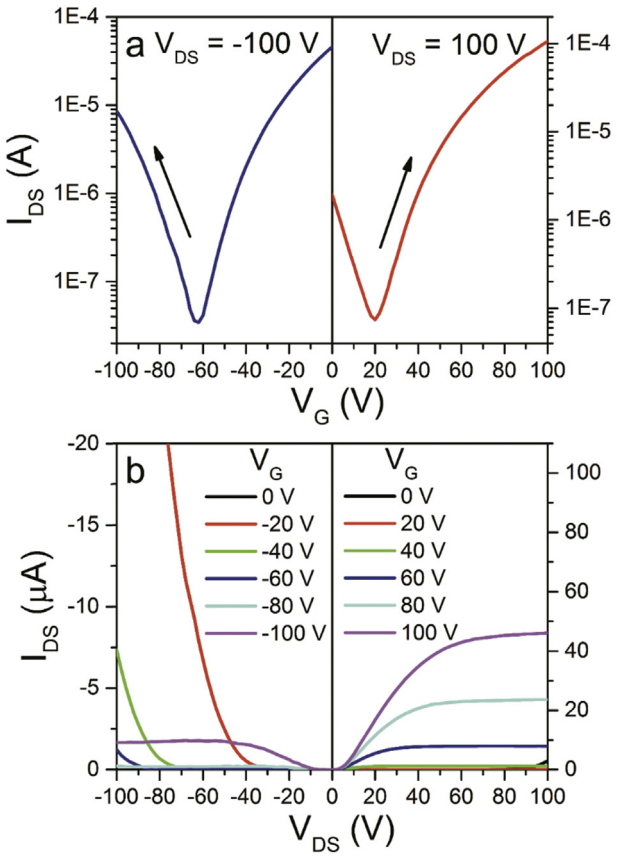

Fig. 3. a) Transfer curves in the p-channel (left) and n-channel (right) operation modes and b) output curves in the p-channel (left) and n-channel (right) operation modes of a typical OTFT device using a **PIBDTBT-40** film annealed at 200 °C as a channel semiconductor. Device dimensions: channel length (L) = 30 μm; channel width (W) = 1 mm.

n^{++}-doped silicon wafer with a 300 nm thermally grown SiO_2 layer as the dielectric and patterned gold pairs as electrodes. Prior to device fabrication, the substrate surface was modified with dodecyltrichlorosilane (DDTS) to minimize the charge traps and improve the polymer chain ordering. The polymer was then spin-coated onto the substrate using a polymer solution in chloroform (5 mg mL^{-1}). Finally, the devices were annealed at 100 °C, 150 °C, 200 °C and 250 °C, respectively, before characterization with an I–V analyser in a nitrogen-filled glove box. All devices showed typical ambipolar charge transport characteristics (Fig. 3). The average hole and electron mobilities for the 100 °C-annealed polymer films are 0.04 $cm^2 V^{-1} s^{-1}$ and 0.06 $cm^2 V^{-1} s^{-1}$, respectively. The mobilities improved as the annealing temperature was increased to 200 °C (Table S2, Supplementary Data). The best electron and hole mobilities are 0.14 $cm^2 V^{-1} s^{-1}$ and 0.10 $cm^2 V^{-1} s^{-1}$, respectively, at this annealing temperature. As the annealing temperature was increased further to 250 °C, the device performance dropped slightly. It is noted that quite well-balanced ambipolar charge transport characteristics (μ_e/μ_h ratio ~1.4) were obtained for this polymer at all annealing temperatures, which is due to its raised HOMO level than that of **PIBDFBT-40** and lowered LUMO level than that of **PIBDPBT-40** as indicated by the CV data.

The polymer thin film crystallinity was investigated with X-ray diffraction (Fig. 4) The polymer thin film annealed at 100 °C showed a primary (100) diffraction peak at $2\theta = 3.02°$, which corresponds to a *d*-spacing distance of 2.92 nm. This is a typical reflection pattern for a crystalline polymer with a layer-by-layer lamellar packing motif [40]. As the annealing temperature was increased to 150 °C, a much stronger primary peak along with a secondary diffraction peak was observed. At a higher annealing temperature of 200 °C, the primary peak continues to intensify and a small peak at 22.81° appeared. This new peak can be assigned to the co-facial π–π stacking distance to be 0.39 nm. Interestingly, as the annealing temperature was increased to 250 °C, this π–π stacking peak disappeared, indicating the polymer chains formed an edge-on orientation [40]. The crystallinity improvement with increasing annealing temperature is in good agreement with improved charge carrier mobilities due to the thermally assisted polymer chain ordering. The atomic force microscopy images of the **PIBDTBT-40** films showed quite smooth surface morphology at all annealing temperatures with a root mean square (RMS) roughness of ~4 nm (Figure S7, Supplementary Data).

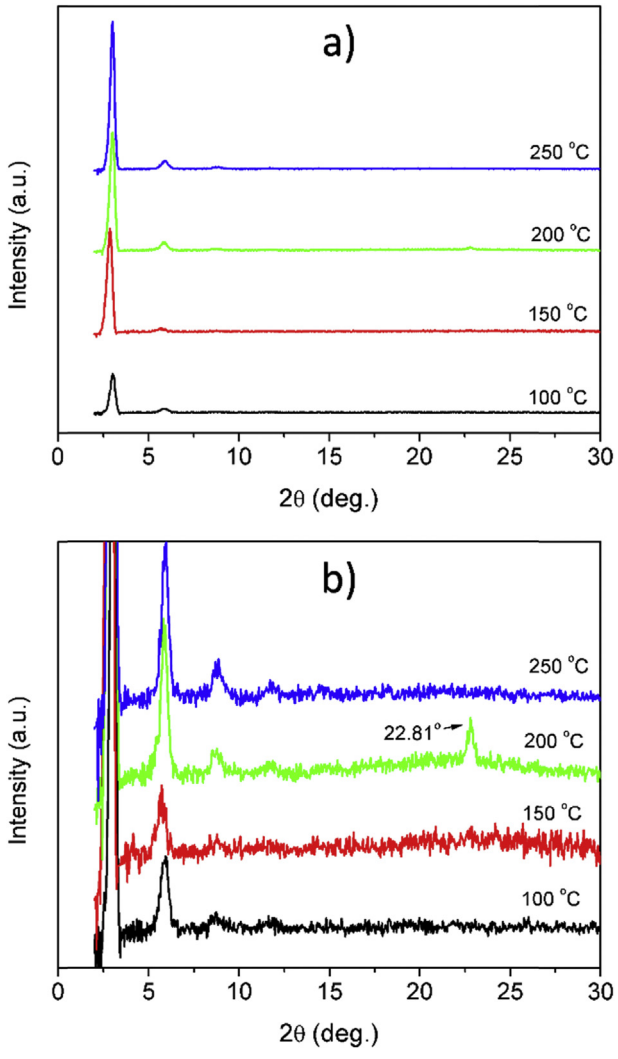

Fig. 4. a) XRD patterns of **PIBDTBT-40** films spin coated on DDTS-modified SiO_2/Si substrates and annealed at different temperatures. b) Zoomed in patterns of a).

3. Methods

3.1. Materials and characterization

All chemicals were purchased from commercial sources and used without further purification. Benzo[1,2-*b*:4,5-*b*′]dithiophene [41] and 6-bromo-1-(4-octadecyldocosyl)indoline-2,3-dione [25] were synthesized according to the literature methods. Computational simulations were performed using density function theory (DFT) calculation with the 6-31G(d) basis set and all the orbital pictures were obtained using GaussView 5.0 software. GPC measurements were performed on a Malvern HT-GPC system using 1,2,4-trichlorobenzene as eluent and polystyrene as standards at 140 °C. TGA measurements were carried out on a TA Instruments SDT 2960 at a scan rate of 10 °C min^{-1} under nitrogen. The UV–Vis–NIR absorption spectra of polymers were recorded on a Thermo Scientific model GENESYS™ 10S VIS spectrophotometer. Cyclic voltammetry (CV) data were obtained on a CHI600E electrochemical analyser using an Ag/AgCl reference electrode with a 0.01 M silver nitrate solution and two Pt disk electrodes as the work and counter electrodes in a 0.1 M tetrabutylammonium hexafluorophosphate solution in anhydrous acetonitrile at a scan rate of 100 mV s^{-1}. Ferrocene was used as the reference, which has a HOMO energy value of −4.8 eV [42]. NMR data was recorded with a Bruker DPX 300 MHz spectrometer with chemical shifts relative to tetramethylsilane (TMS, 0 ppm). Reflection XRD measurements were carried out on a Bruker Smart 6000 CCD 3-circle D8 diffractometer with a Cu RA (Rigaku) X-ray source ($\lambda = 0.15406$ nm). Atomic force microscopy (AFM) images were taken with a Dimension 3100 scanning probe microscope.

3.2. Fabrication and characterization of OTFT devices

The bottom-contact bottom-gate configuration was used for all OTFT devices. The preparation procedure of the substrate and device is as follows. A heavily n-doped SiO_2/Si wafer with ~300 nm-thick SiO_2 was patterned with gold source and drain pairs by conventional photolithography and thermal deposition. Then the substrate was treated with air plasma, followed by cleaning with acetone and isopropanol in an ultra-sonication bath. Subsequently, the substrate was placed in a solution of dodecyltrichlorosilane (DDTS) in toluene (3% in toluene) at room temperature for 20 min, washed with toluene and dried under a nitrogen flow. Then a polymer solution in chloroform (5 mg mL^{-1}) was spin-coated onto the substrate at 3000 rpm for 60 s to give the polymer film, which

was further subject to thermal annealing at different temperatures for 20 min in a glove box. All the OTFT devices have a channel length (L) of 30 μm and a channel width (W) of 1000 μm, and were characterized in the same glove box using an Agilent B2912A Precision Source / Measure Unit.

3.3. Synthetic procedures

3.3.1. Synthesis of benzo[1,2-b:4,5-b′]dithiophene-2,6-diyldiboronic acid (**1**)

To a solution of benzo[1,2-*b*:4,5-*b*']dithiophene (0.22 g, 1.16 mmol) in tetrahydrofuran (15 mL) at −78 °C, n-BuLi (2.5 M in hexanes, 1.84 mL, 4.63 mmol) was added slowly. The reaction mixture was stirred at −78 °C for 2 h, followed by addition of tributyl borate (1.5 mL, 5.56 mmol). The mixture was allowed to reach room temperature and then the solution was stirred overnight. The reaction was quenched by pouring the reaction mixture into water (100 mL) and the mixture was acidified with 10% HCl. The precipitate was collected and re-dissolved with 25% NaOH. Finally it was acidified again with 10% HCl and the precipitated **1** was collected as a white solid, which was used for the next step reaction without further purification. Yield: 0.27 g, 83%.

3.3.2. Synthesis of 3,7-dihydrobenzo[1,2-b:4,5-b′]dithiophene-2,6-dione (**2**)

To a solution of **1** (0.28 g, 1.00 mmol) in THF (15 mL) 30% hydrogen peroxide solution (0.4 mL) was added at room temperature. The reaction mixture was stirred for 45 min and the solvent was removed using a rotavap. The residual was washed with water and methanol to give **2**, which was used for the next step without further purification. Yield: 0.14 g, 61%. ^{1}H NMR (300 MHz, $CDCl_3$) δ 7.29 (s, 2H), 3.99 (s, 4H).

3.3.3. Synthesis of 3,7-bis((E)-6-bromo-1-(4-octadecyldocosyl)-2-oxoindolin-3-ylidene)-3,7-dihydrobenzo[1,2-b:4,5-b′]dithiophene-2,6-dione (**3**)

A solution of **2** (0.13 g, 0.60 mmol) and 6-bromo-1-(4-octadecyldocosyl)indoline-2,3-dione (0.94 g, 1.20 mmol) and *p*-toluenesulfonic acid (24 mg, 0.13 mmol) in toluene (25 mL) was refluxed for 12 h. After cooling down to room temperature the solvent was removed and the residual was purified by silica gel column chromatography using 2:1 hexanes/choloroform to give **3** as a purple solid. Yield: 0.232 g, 22%. ^{1}H NMR (300 MHz, $CDCl_3$) δ 8.71 (s, 2H), 8.33 (d, J = 8.7 Hz), 7.14 (dd, J = 8.4 Hz 1.8 Hz, 2H), 6.90 (d, J = 1.8 Hz, 2H), 3.67 (t, J = 7.4 Hz, 4H), 1.65 (m, 4H), 1.40–1.25 (m, 142H), 0.88 (t, J = 6.6 Hz, 12H). ^{13}C NMR (75 MHz, $CDCl_3$) δ 192.79, 166.56, 146.46, 138.18, 133.97, 133.50, 131.16, 128.90, 125.20, 123.84, 120.35, 111.70, 78.09, 40.74, 37.01, 33.39, 31.82, 30.69, 29.99, 29.60, 29.55, 29.25, 26.57, 24.38, 22.58, 14.03. HR-ESI-MS (M^+) calc. for $C_{106}H_{170}Br_2N_2O_4S_2^+$: 1758.10753; found: 1758.10818.

3.4. Synthesis of PIBDTBT-40

To a 25 mL dry flask was added **3** (58.5 mg, 33.2 μmol) and 5,5′-bis(trimethylstannyl)-2,2′-bithiophene (16.3 mg, 33.2 μmol). After degassing and refilling argon for 3 times, dry chlorobenzene (3 mL) was added. Then a solution of tris(dibenzylideneacetone)-dipalladium ($Pd_2(dba)_3$) (0.6 mg, 2 mol %, 0.665 μmol) and tri(*o*-tolyl) phosphine ($P(o\text{-tolyl})_3$) (0.8 mg, 8 mol %, 2.66 μmol) in anhydrous chlorobenzene (1 mL) was added. The flask was purged with argon for 10 min and sealed. The reaction mixture was stirred at 130 °C for 48 h before cooling down to r.t. The polymer solution was added to methanol (100 mL) and the resulting precipitates were collected by filtration. The polymer was further purified by Soxhlet extraction using acetone and hexanes to remove impurities. Finally the polymer was dissolved in chloroform and re-precipitated in methanol. The solid was collected by filtration and dried to give **PIBDTBT-40**. Yield: 52 mg, 90%.

4. Conclusion

In summary, we reported a novel acceptor building block, IBDT, and an IBDT-based D–A polymer, **PIBDTBT-40**. Compared to its analogous IBDF- and IBDP-based polymers, this IBDT-based polymer has the lowest LUMO level and the smallest exciton binding energy. In OTFTs, this polymer exhibited well-balanced charge transport characteristics with electron mobility up to 0.14 $cm^2\ V^{-1}\ s^{-1}$ and hole mobility up 0.10 $cm^2\ V^{-1}\ s^{-1}$ due to its favorable HOMO and LUMO levels. Our preliminary results indicate that IBDT is a very promising new acceptor building block for D-A polymer semiconductors for ambipolar OTFTs and other printed organic electronics.

Acknowledgements

The authors thank the Natural Sciences and Engineering Research Council (NSERC) of Canada for the financial support (Discovery Grants #402566-2011) of this work.

Appendix A. Supplementary data

Supplementary data related to this article can be found at http://dx.doi.org/10.1016/j.orgel.2016.05.003.

References

[1] A.J. Heeger, Semiconducting polymers: the third generation, Chem. Soc. Rev. 39 (2010) 2354–2371, http://dx.doi.org/10.1039/B914956M.
[2] A.C. Arias, J.D. MacKenzie, I. McCulloch, J. Rivnay, A. Salleo, Materials and applications for large area electronics: solution-based approaches, Chem. Rev. 110 (2010) 3–24, http://dx.doi.org/10.1021/cr900150b.
[3] C. Wang, H. Dong, W. Hu, Y. Liu, D. Zhu, Semiconducting π-conjugated systems in field-effect transistors: a material odyssey of organic electronics, Chem. Rev. 112 (2012) 2208–2267, http://dx.doi.org/10.1021/cr100380z.
[4] K.-J. Baeg, M. Caironi, Y.-Y. Noh, Toward printed integrated circuits based on unipolar or ambipolar polymer semiconductors, Adv. Mater 25 (2013) 4210–4244, http://dx.doi.org/10.1002/adma.201205361.
[5] J.C. Bijleveld, A.P. Zoombelt, S.G.J. Mathijssen, M.M. Wienk, M. Turbiez, D.M. de Leeuw, et al., Poly(diketopyrrolopyrrole–terthiophene) for ambipolar logic and photovoltaics, J. Am. Chem. Soc. 131 (2009) 16616–16617, http://dx.doi.org/10.1021/ja907506r.
[6] Y. Zhao, Y. Guo, Y. Liu, 25th anniversary article: recent advances in n-type and ambipolar organic field-effect transistors, Adv. Mater 25 (2013) 5372–5391, http://dx.doi.org/10.1002/adma.201302315.
[7] B. Sun, W. Hong, Z. Yan, H. Aziz, Y. Li, Record high electron mobility of 6.3 cm 2 V $^{-1}$ s $^{-1}$ achieved for polymer semiconductors using a new building block, Adv. Mater 26 (2014) 2636–2642, http://dx.doi.org/10.1002/adma.201305981.
[8] S.Z. Bisri, C. Piliego, J. Gao, M.A. Loi, Outlook and emerging semiconducting materials for ambipolar transistors, Adv. Mater 26 (2014) 1176–1199, http://dx.doi.org/10.1002/adma.201304280.
[9] Z. Chen, M.J. Lee, R. Shahid Ashraf, Y. Gu, S. Albert-Seifried, M. Meedom Nielsen, et al., High-performance ambipolar Diketopyrrolopyrrole-thieno[3,2-b]thiophene copolymer field-effect transistors with balanced hole and electron mobilities, Adv. Mater 24 (2012) 647–652, http://dx.doi.org/10.1002/adma.201102786.
[10] Y. Li, B. Sun, P. Sonar, S.P. Singh, Solution processable poly(2,5-dialkyl-2,5-dihydro-3,6-di-2-thienyl- pyrrolo[3,4-c]pyrrole-1,4-dione) for ambipolar organic thin film transistors, Org. Electron 13 (2012) 1606–1613, http://dx.doi.org/10.1016/j.orgel.2012.04.023.
[11] B.S. Ong, Y. Wu, P. Liu, S. Gardner, High-performance semiconducting polythiophenes for organic thin-film transistors, J. Am. Chem. Soc. 126 (2004) 3378–3379, http://dx.doi.org/10.1021/ja039772w.
[12] D.M. de Leeuw, M.M.J. Simenon, A.R. Brown, R.E.F. Einerhand, Stability of n-type doped conducting polymers and consequences for polymeric microelectronic devices, Synth. Met. 87 (1997) 53–59, http://dx.doi.org/10.1016/S0379-6779(97)80097-5.
[13] B.A. Jones, A. Facchetti, M.R. Wasielewski, T.J. Marks, Tuning orbital energetics in arylene diimide semiconductors. materials design for ambient stability of n-type charge transport, J. Am. Chem. Soc. 129 (2007) 15259–15278, http://

dx.doi.org/10.1021/ja075242e.
[14] Y. Deng, B. Sun, Y. He, J. Quinn, C. Guo, Y. Li, (3E,8E)-3,8-Bis(2-oxoindolin-3-ylidene)naphtho-[1,2-b:5,6-b[prime or minute]]difuran-2,7(3H,8H)-dione (INDF) based polymers for organic thin-film transistors with highly balanced ambipolar charge transport characteristics, Chem. Commun. 51 (2015) 13515–13518, http://dx.doi.org/10.1039/C5CC03917G.
[15] Y. He, C. Guo, B. Sun, J. Quinn, Y. Li, Branched alkyl ester side chains rendering large polycyclic (3E,7E)-3,7-bis(2-oxoindolin-3-ylidene)benzo[1,2-b:4,5-b[prime or minute]]difuran-2,6(3H,7H)-dione (IBDF) based donor-acceptor polymers solution-processability for organic thin film transistors, Polym. Chem. 6 (2015) 6689–6697, http://dx.doi.org/10.1039/C5PY00782H.
[16] J.D. Yuen, J. Fan, J. Seifter, B. Lim, R. Hufschmid, A.J. Heeger, et al., High performance weak donor–acceptor polymers in thin film transistors: effect of the acceptor on electronic properties, ambipolar conductivity, mobility, and thermal stability, J. Am. Chem. Soc. 133 (2011) 20799–20807, http://dx.doi.org/10.1021/ja205566w.
[17] J.D. Yuen, F. Wudl, Strong acceptors in donor-acceptor polymers for high performance thin film transistors, Energy Environ. Sci. 6 (2013) 392–406, http://dx.doi.org/10.1039/C2EE23505F.
[18] Z. Yan, B. Sun, Y. Li, Novel stable (3E,7E)-3,7-bis(2-oxoindolin-3-ylidene) benzo[1,2-b:4,5-b[prime or minute]]difuran-2,6(3H,7H)-dione based donor-acceptor polymer semiconductors for n-type organic thin film transistors, Chem. Commun. 49 (2013) 3790–3792, http://dx.doi.org/10.1039/C3CC40531A.
[19] H. Yan, Z. Chen, Y. Zheng, C. Newman, J.R. Quinn, F. Dötz, et al., A high-mobility electron-transporting polymer for printed transistors, Nature 457 (2009) 679–686, http://dx.doi.org/10.1038/nature07727.
[20] H. Li, F.S. Kim, G. Ren, S.A. Jenekhe, High-mobility n-type conjugated polymers based on electron-deficient tetraazabenzodifluoranthene diimide for organic electronics, J. Am. Chem. Soc. 135 (2013) 14920–14923, http://dx.doi.org/10.1021/ja407471b.
[21] H. Usta, C. Newman, Z. Chen, A. Facchetti, Dithienocoronenediimide-based copolymers as novel ambipolar semiconductors for organic thin-film transistors, Adv. Mater 24 (2012) 3678–3684, http://dx.doi.org/10.1002/adma.201201014.
[22] Y. He, W. Hong, Y. Li, New building blocks for π-conjugated polymer semiconductors for organic thin film transistors and photovoltaics, J. Mater. Chem. C 2 (2014) 8651–8661, http://dx.doi.org/10.1039/C4TC01201A.
[23] X. Guo, M. Baumgarten, K. Müllen, Designing π-conjugated polymers for organic electronics, Prog. Polym. Sci. 38 (2013) 1832–1908, http://dx.doi.org/10.1016/j.progpolymsci.2013.09.005.
[24] C. Guo, W. Hong, H. Aziz, Y. Li, Recent progress in high mobility polymer semiconductors for organic thin film transistors, Rev. Adv. Sci. Eng. 1 (2012) 200–224, http://dx.doi.org/10.1166/rase.2012.1014.
[25] T. Lei, J.-H. Dou, X.-Y. Cao, J.-Y. Wang, J. Pei, Electron-deficient poly(p-phenylene vinylene) provides electron mobility over 1 cm2 V−1 s−1 under ambient conditions, J. Am. Chem. Soc. 135 (2013) 12168–12171, http://dx.doi.org/10.1021/ja403624a.
[26] T. Lei, J.-H. Dou, X.-Y. Cao, J.-Y. Wang, J. Pei, A BDOPV-based donor-acceptor polymer for high-performance n-type and oxygen-doped ambipolar field-effect transistors, Adv. Mater 25 (2013) 6589–6593, http://dx.doi.org/10.1002/adma.201302278.
[27] G. Zhang, P. Li, L. Tang, J. Ma, X. Wang, H. Lu, et al., A bis(2-oxoindolin-3-ylidene)-benzodifuran-dione containing copolymer for high-mobility ambipolar transistors, Chem. Commun. 50 (2014) 3180, http://dx.doi.org/10.1039/c3cc48695h.
[28] T. Lei, X. Xia, J.-Y. Wang, C.-J. Liu, J. Pei, "Conformation Locked" strong electron-deficient poly(p-phenylene vinylene) derivatives for ambient-stable n-type field-effect transistors: synthesis, properties, and effects of fluorine substitution position, J. Am. Chem. Soc. 136 (2014) 2135–2141, http://dx.doi.org/10.1021/ja412533d.
[29] X. Zhou, N. Ai, Z.-H. Guo, F.-D. Zhuang, Y.-S. Jiang, J.-Y. Wang, et al., Balanced ambipolar organic thin-film transistors operated under ambient conditions: role of the donor Moiety in BDOPV-based conjugated copolymers, Chem. Mater 27 (2015) 1815–1820, http://dx.doi.org/10.1021/acs.chemmater.5b00018.
[30] Y. He, C. Guo, B. Sun, J. Quinn, Y. Li, (3E,7E)-3,7-Bis(2-oxoindolin-3-ylidene)-5,7-dihydropyrrolo[2,3-f]indole-2,6(1H,3H)-dione based polymers for ambipolar organic thin film transistors, Chem. Commun. 51 (2015) 8093–8096, http://dx.doi.org/10.1039/C5CC01021G.
[31] Y. Cao, J.-S. Yuan, X. Zhou, X.-Y. Wang, F.-D. Zhuang, J.-Y. Wang, et al., N-Fused BDOPV: a tetralactam derivative as a building block for polymer field-effect transistors, Chem. Commun. 51 (2015) 10514–10516, http://dx.doi.org/10.1039/C5CC02026C.
[32] M. Nakatsuka, K. Nakasuji, I. Murata, I. Watanabe, G. Saito, T. Enoki, et al., 3,7-dihalo-2H,6H-benzo(1,2-b:4,5-b′)dithiophene-2,6-dione. New Wurster-type acceptors isoelectronic with 2,6-anthraquinone, Chem. Lett. (1983) 905–908, http://dx.doi.org/10.1246/cl.1983.905.
[33] E.A. Castro, Kinetics and mechanisms of reactions of thiol, thiono, and dithio analogues of carboxylic esters with nucleophiles, Chem. Rev. 99 (1999) 3505–3524, http://dx.doi.org/10.1021/cr990001d.
[34] P.M. Beaujuge, C.M. Amb, J.R. Reynolds, Spectral engineering in π-conjugated polymers with intramolecular donor–acceptor interactions, Acc. Chem. Res. 43 (2010) 1396–1407, http://dx.doi.org/10.1021/ar100043u.
[35] F.C. Spano, The spectral signatures of Frenkel Polarons in H- and J-aggregates, Acc. Chem. Res. 43 (2010) 429–439, http://dx.doi.org/10.1021/ar900233v.
[36] J. Shin, H.A. Um, D.H. Lee, T.W. Lee, M.J. Cho, D.H. Choi, High mobility isoindigo-based π-extended conjugated polymers bearing di(thienyl)ethylene in thin-film transistors, Polym. Chem. 4 (2013) 5688, http://dx.doi.org/10.1039/c3py00735a.
[37] N.S. Sariciftci, Primary Photoexcitations in Conjugated Polymers: Molecular Exciton versus Semiconductor Band Model, World Scientific, 1997.
[38] Y. Zhu, R.D. Champion, S.A. Jenekhe, Conjugated donor–acceptor copolymer semiconductors with large intramolecular charge transfer: synthesis, optical properties, electrochemistry, and field effect carrier mobility of thienopyrazine-based copolymers, Macromolecules 39 (2006) 8712–8719, http://dx.doi.org/10.1021/ma061861g.
[39] L.J.A. Koster, S.E. Shaheen, J.C. Hummelen, Pathways to a new efficiency regime for organic solar cells, Adv. Energy Mater 2 (2012) 1246–1253, http://dx.doi.org/10.1002/aenm.201200103.
[40] H. Sirringhaus, P.J. Brown, R.H. Friend, M.M. Nielsen, K. Bechgaard, B.M.W. Langeveld-Voss, et al., Two-dimensional charge transport in self-organized, high-mobility conjugated polymers, Nature 401 (1999) 685–688.
[41] T. Kashiki, S. Shinamura, M. Kohara, E. Miyazaki, K. Takimiya, M. Ikeda, et al., One-pot synthesis of benzo[b]thiophenes and benzo[b]selenophenes from o-halo-substituted ethynylbenzenes: convenient approach to mono-, bis-, and tris-chalcogenophene-annulated benzenes, Org. Lett. 11 (2009) 2473–2475, http://dx.doi.org/10.1021/ol900809w.
[42] J. Pommerehne, H. Vestweber, W. Guss, R.F. Mahrt, H. Bassler, M. Porsch, et al., Efficient two layer leds on a polymer blend basis, Adv. Mater 7 (1995) 551–554, http://dx.doi.org/10.1002/adma.19950070608.